Propellants, Explosives, Pyrotechnics 15, 81–86 (1990)

Thermal Decomposition of Energetic Materials
41. Fast Thermolysis of Cyclic and Acyclic Ethanediammonium Dinitrate Salts and their Oxonium Nitrate Double Salts, and the Crystal Structure of Piperazinium Dinitrate

T. P. Russell, T. B. Brill*, A. L. Rheingold, and B. S. Haggerty

Department of Chemistry, University of Delaware, Newark, DE 19716 (USA)

Thermische Zersetzung von energiereichen Verbindungen. 41. Schnelle Thermolyse von cyclischen und acyclischen Ethandiammoniumdinitrat-Salzen und ihrer Oxoniumnitrat-Doppelsalze; Kristallstruktur von Piperaziniumdinitrat

Schnelle Thermolyse verbunden mit FTIR-Spektroskopie wird beschrieben von $[H_3NCH_2CH_2NH_3](NO_3)_2$ (EDD), $[H_2N(CH_2CH_2)_2NH_2](NO_3)_2$ (PIPDN) und $[HN(CH_2CH_2)_3NH](NO_3)_2$ (DABCOD), desgleichen von den neuen Oxoniumnitrat-Doppelsalzen des PIPDN und DABCOD. Beim Erhitzen ≥ 100 °C liefert EDD zu Beginn HNO_3, dann kleine molekulare Zersetzungsprodukte aus den Redox-Reaktionen. PIPDN spaltet ebenfalls zu Beginn HNO_3 ab, bildet dann aber eine beträchtliche Menge an N,N'-Dinitrosopiperazin zusammen mit kleinen molekularen Spaltprodukten. DABCOD bildet keine gasförmige HNO_3 aber stattdessen CH_2O, N,N'-Dinitrosopiperazin und kleine Moleküle. Diese Modelle sind ganz in Übereinstimmung mit dem Verhalten, das in unserer früheren Arbeit für primäre, sekundäre und tertiäre Ammoniummononitratsalze beobachtet wurde. Die Entstehung von Nitrosaminen als Thermolyseprodukte läßt das Gesundheitsrisiko dieser Materialien stark ansteigen. Nitramine als Thermolyseprodukte wurden nicht nachgewiesen. Bei der Thermolyse der Oxoniumnitrat-Doppelsalze wird HNO_3 und H_2O frei bei einer relativ niedrigen Temperatur (~ 60 °C). Oberhalb dieser Temperatur verläuft die Thermolyse in derselben Weise wie bei reinem PIPDN und DABCOD. Die Kristallstruktur von PIPDN wird beschrieben.

Décomposition thermique des compositions riches en énergie. 41. Thermolyse rapide de sels de dinitrate de diammoniuméthane cycliques et acycliques et de leurs sels doubles de nitrate d'oxonium; structure cristalline du dinitrate de piperazinium

On décrit la thermolyse rapide associée à la spectroscopie IR par transformée de Fourier (FTIR) des composés $[H_3NCH_2CH_2NH_3](NO_3)_2$ (EDD), $[H_2N(CH_2CH_2)_2NH_2](NO_3)_2$ (PIPDN) et $[HN(CH_2CH_2)_3NH](NO_3)_2$ (DABCOD), ainsi que des nouveaux sels doubles du nitrate d'oxonium du PIPDN et du DABCOD. Lors de la montée en température jusqu'à 100 °C, EDD donne d'abord lieu à un dégagement de HNO_3, puis des produits de décomposition à molécules de faible taille, résultant de réactions d'oxydo-réduction. PIPDN dégage également en premier lieu HNO_3 mais produit ensuite une quantité importante de N,N'-dinitrosopipérazine ainsi que des produits de décomposition à molécules de petite taille. DABCOD ne donne pas lieu à un dégagement de HNO_3 gazeux mais produit CH_2O, N,N'-dinitrosopipérazine et de petites molécules. Ces modèles de décomposition concordent bien avec le comportement des mononitrates d'ammonium primaires, secondaires et tertiaires décrit dans une étude antérieure. Du fait de l'apparition de nitrosamines comme produits de la thermolyse, le risque toxique que présentent ces substances croît considérablement. On n'a pas pu déceler de nitrosamines parmi les produits de la thermolyse. La thermolyse des sels doubles de nitrate d'oxonium donne lieu, à température relativement basse (env. 60 °C) à un dégagement de HNO_3 et de H_2O. Aux températures supérieures, la thermolyse se déroule suivant le même schéma que pour le PIPDN et le DABCOD. On décrit par ailleurs la structure cristalline du PIPDN.

Summary

Fast thermolysis/FTIR spectroscopy of $[H_3NCH_2CH_2NH_3](NO_3)_2$ (EDD), $[H_2N(CH_2CH_2)_2NH_2](NO_3)_2$ (PIPDN), and $[HN(CH_2CH_2)_3NH](NO_3)_2$ (DABCOD) and new oxonium nitrate ($H_3O^+NO_3^-$) double salts of PIPDN and DABCOD is described. EDD initially yields HNO_3 and then small molecule decomposition products from redox reactions when heated at ≥ 100 °C (dec.). PIPDN initially yields HNO_3, but then generates a significant amount of N,N'-dinitrosopiperazine along with small molecule fragments. DABCOD produces no $HNO_3(g)$, but instead gives CH_2O, N,N'-dinitrosopiperazine and small molecule products. These patterns are entirely consistent with the behavior observed for primary, secondary and tertiary ammonium mononitrate salts in our previous work. The presence of nitrosamines strongly increases the health hazard of the materials upon heating. No nitramines were detected as thermolysis products. Thermolysis of the oxonium nitrate double salts liberates HNO_3 and H_2O at a relatively low temperature (~ 60 °C). Above this temperature, the thermolysis proceeds in the same way as that of pure PIPDN and DABCOD. The crystal structure of PIPDN is described.

1. Introduction

As part of a project to develop structure/property/thermolysis relationships for alkylammonium nitrate salts⁽¹⁾, we investigated the series of ethanediammonium cations having the stoichiometry $[H_{1+n}N(CH_2CH_2)_{3-n}NH_{1+n}]^+$, n = 0, 1, 2. This series permits the effect of chain, ring and cage incorporation of the amine to be characterized. EDD is ethanediammonium dinitrate, PIPDN is piperazinium dinitrate, and DABCOD is diazabicyclo[2.2.2]octane dinitrate. EDD is well known as a component of explosive formulations⁽²⁾. Hence, the fast thermal decomposition reactions of these compounds have practical interest.

During the synthesis of EDD, PIPDN and DABCOD, it was discovered that PIPDN and DABCOD could be precipitated as double salts having the stoichiometry

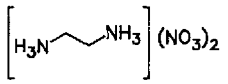

EDD

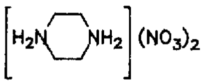

PIPDN

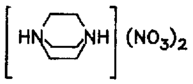

DABCOD

---

* Correspondence author.

0721-3115/90/0306-0081$3.50+.25/0

PIPDN · H_3O · NO_3 and DABCOD · H_3O · NO_3. However, attempts to grow crystals of the double salts having diffraction quality by slow crystallization led only to the simple salts, PIPDN and DABCOD. The crystal structure of PIPDN was determined by single crystal X-ray diffraction. Fast thermal decomposition of EDD, PIPDN, PIPDN · H_3O · NO_3, DABCOD, and DABCOD · H_3O · NO_3 was determined by the temperature profiling/FTIR method(3).

2. Experimental

2.1 Synthesis

EDD was prepared by adding 6 M HNO_3 to a cold aqueous solution of ethanediamine. The precipitate was removed by filtration and dried at 1×10^{-2} torr for 8–12 h. PIPDN and DABCOD were prepared by adding a slight excess of HNO_3 to the amine in ethanol. The precipitate was removed by filtration and dried at 1×10^{-4} torr for 8–12 h. PIPDN · H_3O · NO_3 and DABCOD · H_3O · NO_3 were prepared as described above for the PIPDN and DABCOD salts except that HNO_3 was added until a pH of 1.5–2 was reached. The precipitate was filtered and dried for 8–12 hrs at 1×10^{-2} torr. Elemental analysis confirmed the stoichiometries of the salts as given.

To verify that the cations were unaffected by the nitration reaction leading to the putative double salts, the ^1H NMR spectra were recorded in D_2O on a Bruker AM-250 spectrometer. A single peak for PIPDN and PIPDN · H_3O · NO_3 appeared at 5.90 ppm (relative to H_2O), while DABCOD and DABCOD · H_3O · NO_3 produced a single peak at 6.25 ppm. Thus, no disturbance of the cation backbone occurred during the addition of excess HNO_3.

2.2 Titration of the total acid present

Further proof of double salt formation was gained by the titration of these salts with 0.04 M NaOH. The double salts were found to contain 3.00 ± 0.01 equivalents of H^+ while the simple salts contained 2.00 ± 0.02 equivalents of H^+. The first equivalent of acid of each double salt titrated as a strong acid, while the second and third titrated as moderately weak acids. The second and third end points of the double salts matched the first and second end points of the simple salts.

2.3 Fast thermolysis/FTIR spectroscopy

The temperature profiling/FTIR method has been described elsewhere(3). In general, 1–2 mg of sample was thinly spread on the Nichrome ribbon filament of the cell. The Ar pressure was adjusted as described in the 2–1000 psi range (1 psi ≅ 6.9 kPa), but only selected results are described in this paper. Real-time temperature measurements of the condensed phase were made simultaneously with rapid-scan IR detection of the evolved gases several mm above the surface of the sample. A Nicolet 60 SX FTIR spectrometer set at 4 cm^{-1} resolution, 10 scans/s, and 2 spectra per file was used to record these data. The relative percent composition versus time profiles were constructed from the peak heights and the known absolute intensities for most of the gases(4). H_2O was detected, but not quantified, because of the complex rotation-vibration fine structure. Authentic samples of N,N′-dinitrosopiperazine (Aldrich), N,N′-dinitropiperazine (H. G. Adolph, NSWC, White Oak, MD) and piperazine (Aldrich) were used to verify that thermolysis of DIPDN and DABCOD liberated these products upon fast thermolysis.

2.4 TGA/DSC measurements

Thermogravimetric analysis and differential scanning calorimetry were performed on a DuPont Instruments 2000 analyzer equipped with a 951 TGA cell and a 910 DSC cell. 2–5 mg of sample were used and the heating rate was 5–10 °C/min. For TGA measurements, an N_2 flow rate of 75 ml/min was present.

2.5 X-Ray crystallography

Diffraction quality crystals were produced by slow crystallization from the mother liquor. Unfortunately, only the simple salts, PIPDN and DABCOD crystallized when the double salt was added. Hence, only the structure of PIPDN was determined.

A colorless crystal of PIPDN was mounted on a glass fiber with epoxy cement. The unit cell parameters (Table 1) were determined from the least squares fit of 25 reflections in the range of $20° \leq 2\,\theta \leq 25°$. The parameters used during the collection of the diffraction data are contained in Table 1. An absorption correction was not needed ($\mu = 1.92\ cm^{-1}$). The space group was changed from a C-centered to an I-centered lattice to reduce the β-angle; the I2/a space group was confirmed through the results of refinement.

The structure was solved by direct methods which located all of the non-hydrogen atoms. Subsequent least squares and difference Fourier calculations located all of the hydrogen atoms. C, N and O were refined anisotropically(5). The atomic coordinates are given in Table 2.

3. Crystal Structure of PIPDN

The crystal structure of PIPDN is shown in Fig. 1. The packing of the lattice is determined by N–H···O hydrogen bonding involving each oxygen atom. Figure 2 shows the unique intermolecular interactions in more detail. One of

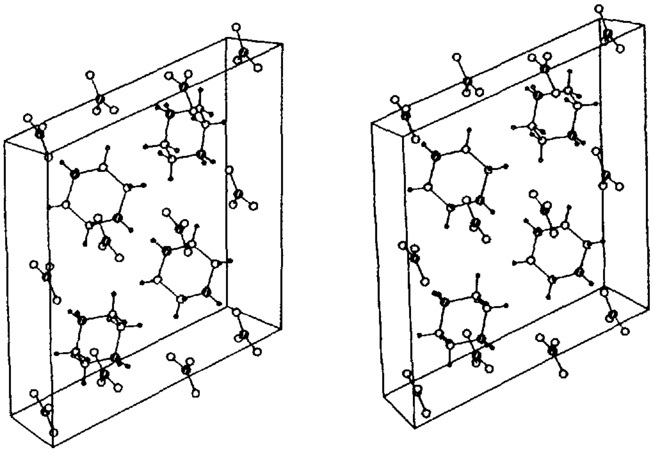

Figure 1. The unit cell of PIPDN viewed along the b axis.

Table 1. Crystal, Collection and Refinement Data for PIPDN

	(a) Crystal Data		
formula	$C_4H_{12}N_4O_6$	V, Å^3	935.9(6)
formula wt.	212.1	Z	4
crystal system	monoclinic	μ(MoKα), cm^{-1}	1.92
space group	$I2/a$	D (calcd, g/cm^3)	1.505
a, Å	12.446(4)	temp, K	296
b, Å	5.944(2)	crystal size, mm	0.18 × 0.23 × 0.42
c, Å	13.554(4)	crystal color	colorless
β, deg.	111.05(2)		
	(b) Data Collection		
diffractometer	Nicolet R3m	data collected	±17, +8, +18
monochromator	graphite	rflns collected	1224
radiation	MoKα		
wavelength, Å	0.71073	R(int), %	0.94
scan method	Wyckoff	indpt rflns	756
scan limits, deg	$4 \leq 2\theta \leq 55$	$F_o \geq 5\,\sigma(F_o)$	
	(c) Refinements Results		
R_F %	4.17	Δ(p), eÅ^{-3}	0.191
R_{wF} %	4.85	N_o/N_v	8.49
Δ/σ (max)	0.001	GOF	1.310

Table 2. Atomic Coordinates (× 10^4) and Isotropic Thermal Parameters (Å^2 × 10^3)

	x	y	z	U
N(1)	6694(2)	2022(3)	6460(1)	43(1)*
N(2)	6176(1)	-2979(3)	5119(1)	40(1)*
O(1)	5960(1)	-1073(3)	4715(1)	56(1)*
O(2)	6561(1)	-3152(3)	6105(1)	58(1)*
O(3)	5983(1)	-4685(3)	4557(1)	68(1)*
C(1)	6367(2)	1682(4)	7406(2)	43(1)*
C(2)	7958(2)	1716(4)	6725(2)	47(1)*
Hne	6328(19)	1103(41)	5964(18)	52(6)
Hna	6476(25)	3482(49)	6184(22)	75(8)

* Equivalent isotropic U defined as one third of the trace of the orthogonalized U_{ij} tensor.

Table 3. Bond Distances (Å) for PIPDN

N(1)-C(1)	1.491(3)	N(1)-C(2)	1.494(3)
N(1)-Hne	0.859(22)	N(1)-Hna	0.945(29)
N(2)-O(1)	1.245(2)	N(2)-O(2)	1.252(2)
N(2)-O(3)	1.238(2)	C(1)-H(1E)	0.915(25)
C(1)-H(1A)	0.991(24)	C(1)-C(2A)	1.512(3)
C(2)-H(2E)	0.950(33)	C(2)-H(2A)	0.990(23)
C(2)-C(1A)	1.512(3)		

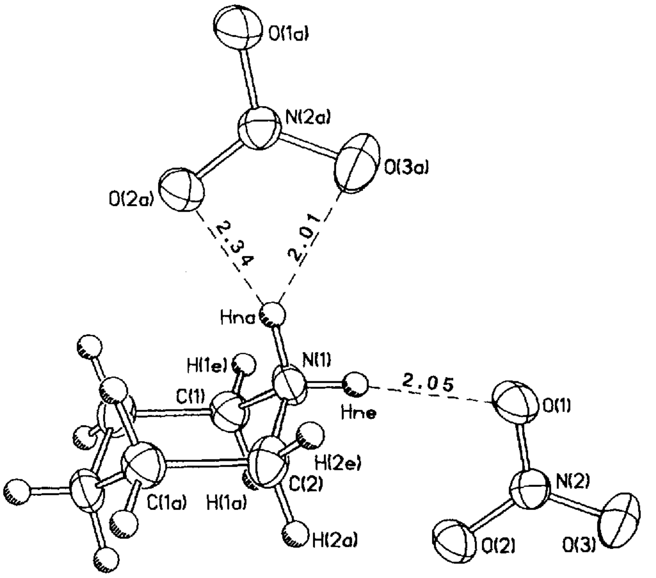

Figure 2. The unique hydrogen bonds found in the PIPDN lattice. 40 percent probability ellipsoids are shown for the non-hydrogen atoms.

Table 4. Bond Angles (°) for PIPDN

C(1)-N(1)-C(2)	111.5(1)	C(1)-N(1)-Hne	110.8(18)
C(2)-N(1)-Hne	109.1(17)	C(1)-N(1)-Hna	109.6(21)
C(2)-N(1)-Hna	109.6(19)	Hne-N(1)-Hna	106.2(22)
O(1)-N(2)-O(2)	118.9(2)	O(1)-N(2)-O(3)	120.8(2)
O(2)-N(2)-O(3)	120.3(2)	N(1)-C(1)-H(1E)	106.2(17)
N(1)-C(1)-H(1A)	105.4(15)	H(1E)-C(1)-H(1A)	112.5(18)
N(1)-C(1)-C(2A)	109.7(2)	H(1E)-C(1)-C(2A)	110.8(14)
H(1A)-C(1)-C(2A)	111.9(11)	N(1)-C(2)-H(2E)	106.0(16)
N(1)-C(2)-H(2A)	106.5(14)	H(2E)-C(2)-H(2A)	112.0(21)
N(1)-C(2)-C(1A)	110.6(2)	H(2E)-C(2)-C(1A)	109.6(14)
H(2A)-C(2)-C(1A)	111.8(11)		

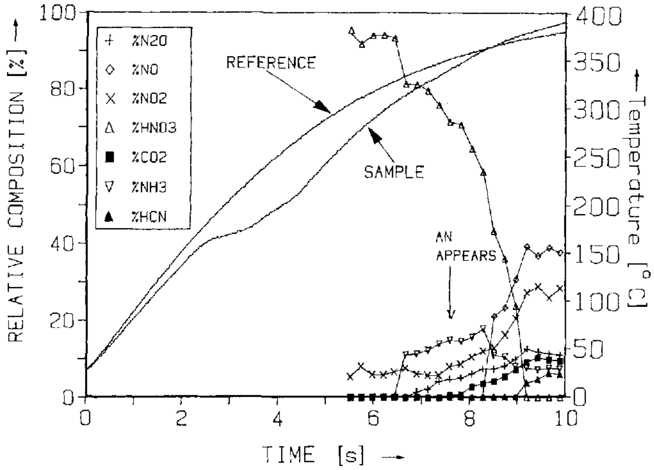

Figure 3. The relative percent composition of the evolved gases and temperature profile of the condensed phase for 1 mg of EDD rapidly heated under 15 psi Ar.

the N-H···O hydrogen bonds is bifurcated. The intramolecular bond distances (Table 3) and angles (Table 4) are regular and normal. The piperidinium ion adopts the chair conformation. The extensive amount of hydrogen bonding contributes to the thermal decomposition characteristics of these salts through the release $HNO_3(g)$ in the initial decomposition step.

4. Thermal Decomposition

4.1 EDD

Fast thermolysis/FTIR results for EDD have been described before[(6)] and so only several pertinent observations will be mentioned. As shown in Fig. 3, EDD melts at about 180 °C. HNO_3 and NO_2 are the initial gas products detected at about 275 °C. NO_2 probably forms from the thermal decomposition of HNO_3. NH_3 appears at about 300 °C indicating C–N bond fission and $H^{\cdot}$ migration occurs. The sample heating rate slows somewhat during these HNO_3 and NH_3 evolution steps indicating the net endothermicity of these processes. The reaction of HNO_3 with NH_3 in the gas phase produces an NH_4NO_3 aerosol which is detected at about 310 °C. The reduction of HNO_3/NO_2 to NO and the oxidation of the hydrocarbon residue to CO/CO_2 occurs at about 330 °C and is exothermic. Thus, under the conditions of this experiment, the initiation step is the proton transfer reaction. Subsequent reactions lead to destruction of the residue and the formation of small molecule gases. There are no volatile products that indicate coupling reactions involving ethanediamine molecules, nor is ethanediamine evolved under these heating conditions. It has been suggested that nitramine and nitrosamine containing compounds form during the thermal decomposition of EDD[(7)], but there was no direct evidence of these products under the experimental conditions used here. Because the decomposition temperature of 1,2-ethanedinitramine is substantially below the temperature at which the gas products appear from EDD[(1)], it seems unlikely that any primary nitramines could have formed.

4.2 PIPDN

By TGA, weight loss begins at about 240 °C. This corresponds to an exotherm by DSC at about 235 °C. Unlike EDD, the sample does not melt. As shown in Fig. 4, fast heating of PIPDN at 15 psi liberates HNO_3 and a small amount of NO_2 beginning at about 260 °C. Trace amounts of CO_2 and N_2O are detected in the 275 °C–290 °C range indicating the occurrence of a small amount of backbone oxidation. PIPDN aerosol is detected at about 310 °C indicating that piperazine (PIP) must be thermally stable enough to evolve intact to the gas phase where it recombines with HNO_3. In fact, when the thermolysis of PIPDN is conducted at 2 psi Ar, free PIP appears in the gas phase. This contrasts with EDD, where no ethanediamine or EDD can be detected in the gas phase. Instead, EDD decomposes to liberate NH_3 which forms AN aerosol. Also liberated from PIPDN thermolysis in the 310 °C range is N,N'-dinitrosopiperazine (DNOP). The occurrence of DNOP is understandable from the fact that thermolysis of dialkylammonium nitrate salts produce the dialkylnitrosamine among the products[(1)]. NO is detected in the same temperature range as DNOP. The high vapor pressure of an

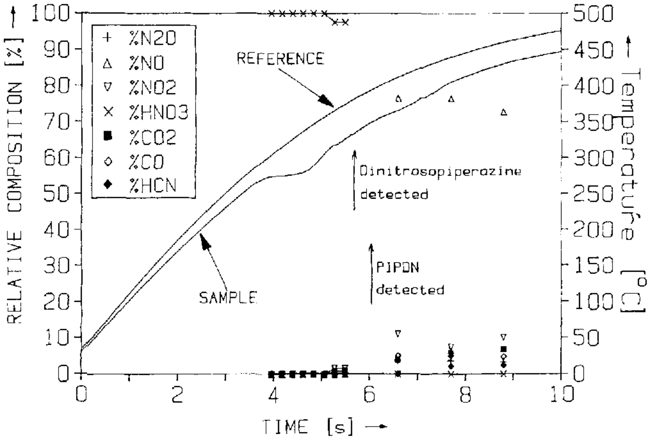

Figure 4. The relative percent composition of the evolved gases and the temperature profile of the condensed phase for 1 mg of PIPDN rapidly heated under 15 psi Ar.

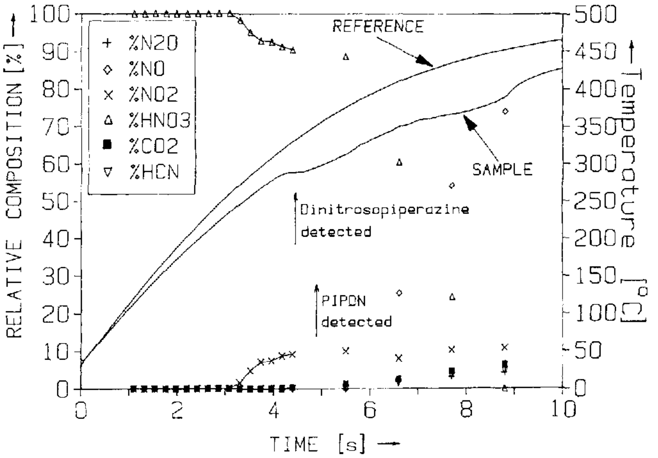

Figure 5. The relative percent composition of the evolved gases and the temperature profile of the condensed phase for 1 mg of PIPDN · H_3O · NO_3 heated under 15 psi Ar.

authentic sample of DNOP and the N–NO bond homolysis pathway of decomposition[8] explain these observations.

It was not established by this work how DNOP forms from PIPDN. However, DNOP does not appear to be formed via N,N'-dinitropiperazine (DNP), even though piperazine and HONO are known to react to form DNP[9]. If DNP were to form, DNOP might be a thermolysis product because nitrosamines can form during the thermal decomposition of nitramines[10, 11]. However, we find that an authentic sample of DNP readily sublimes on heating and that its vapor pressure is sufficiently large even under 1000 psi Ar to allow ready detection of DNP(g) by IR spectroscopy. Thus, if DNP had formed in the fast thermolysis of PIPDN, we should detect DNP in the gas phase, which we do not. Therefore, it is probable that DNOP forms from PIPDN without passing through a DNP intermediate.

4.3 PIPDN · $H_3O \cdot NO_3$

Two irreversible endotherms in the 95 °C–125 °C range appear in the DSC of this compound which, by TGA, correspond to the loss of $H_2O \cdot HNO_3$. Above this temperature range, the thermochemistry of the residue resembles that of PIPDN discussed above. These observations are supported by fast thermolysis/FTIR studies. Figure 5 shows that HNO_3 appears in the gas phase beginning at about 110 °C. NO_2 from the thermal decomposition of HNO_3 is detected at about 235 °C. If thermalized at 2 psi, PIP can be detected in the gas phase. DNOP is detected beginning at about 290 °C and there is no evidence of DNP.

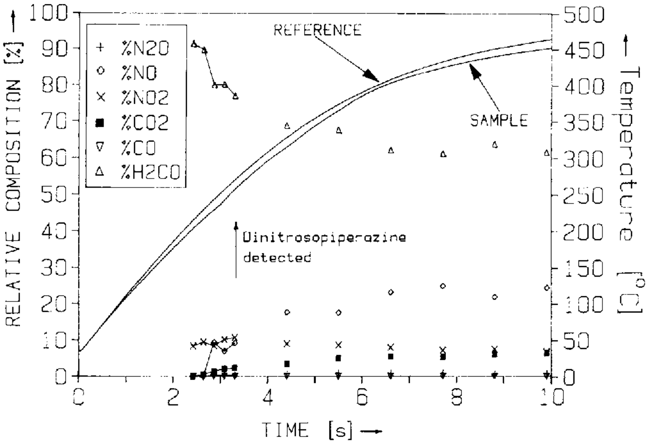

Figure 6. The relative percent composition of the evolved gases and the temperature profile of the condensed phase for 1 mg of DABCOD heated under 15 psi Ar.

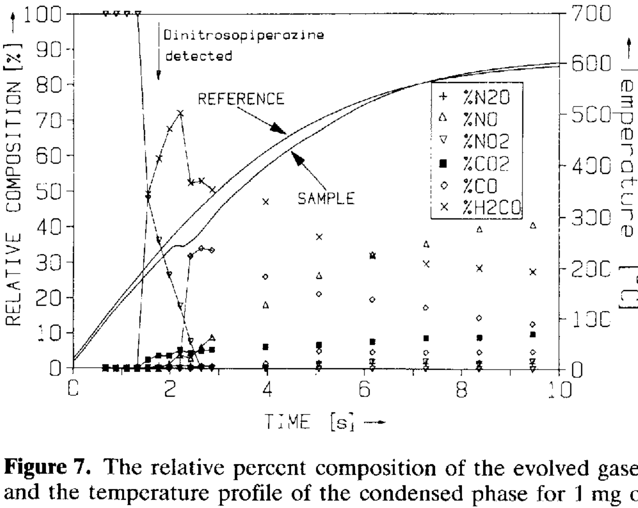

Figure 7. The relative percent composition of the evolved gases and the temperature profile of the condensed phase for 1 mg of DABCOD · $H_3O \cdot NO_3$ rapidly heated under 15 psi Ar.

4.4 DABCOD

No melting endotherm was detected in any experiment on DABCOD. A decomposition exotherm occurred by DSC at 172 °C which corresponds to a weight loss by TGA beginning at 175 °C. These results are given more detail by the fast thermolysis/FTIR measurements shown in Fig. 6. Unlike the primary and secondary alkylammonium nitrate salts discussed above, no HNO_3 is released to the gas phase either at the onset of decomposition or in the later stages. In fact, no tertiary alkylammonium nitrate salts studied in our work[1] liberate HNO_3 upon fast thermolysis. However, it seems probable that HNO_3 may form in the condensed phase because NO_2 and NO are found, but that it instantly reacts with the amine before it is released from the condensed phase. α-Carbon oxidation occurs to produce CH_2O and DNOP along with other products. The thermolysis of DABCOD has been reported before to produce DNOP[12]. Also the radical cation of DABCOD decomposes by C–C scission[13]. This type of reaction appears to be broadly applicable to tertiary alkylammonium nitrate salts. For instance, the fast thermolysis of trimethylammonium nitrate, no HNO_3 is detected and N,N-dimethylformamide is generated[1]. In the case of DABCOD, the reaction cleaves two C–N bonds to destroy the cage structure and oxidize two α-carbon atoms to CH_2O. The reaction ceases after one step leaving the piperazine ring which is then converted to DNOP. DNOP is apparently the relatively stable and volatile intermediate formed in the decomposition scheme of DABCOD (as well as for PIPDN).

4.5 DABCOD · $H_3O \cdot NO_3$

This double salt displays an irreversible endotherm 100 °C–108 °C by DSC corresponding to a weight loss of $H_2O \cdot HNO_3$ by TGA. Fast thermolysis/FTIR results are shown in Fig. 7. As expected, the decomposition of the residue above this temperature closely resembles that of DABCOD discussed above because the sample has transformed to pure DABCOD at this point.

5. General Patterns

The initial thermal decomposition step of the rapidly heated acyclic primary (EDD) and monocyclic secondary (PIPDN) diammonium dinitrate salts is the formation and release of a portion of the HNO_3 to the gas phase. The bicyclic tertiary diammonium dinitrate salt (DABCOD) does not release HNO_3 to the gas phase, but, instead, consumes HNO_3 immediately in the condensed phase through α-carbon oxidation and secondary nitrosamine formation. This latter reaction may be favored because of the opportunity to gain some double bond character through secondary nitrosamine formation. The onset of thermal decomposition is controlled by the above initiation steps. For EDD and PIPDN, the initial step is the formation and desorption of HNO_3, which occurs in the 260 °C–275 °C range at 15 psi when rapidly heated. On the other hand, DABCOD is controlled by the temperature at which the cage opens. Thus, it begins to decompose at a different temperature (190 °C–210 °C).

Following the formation of HNO_3 from the primary diammonium dinitrate salt (EDD), the next major step in the reaction scheme is opening of the chain by C–N bond fission to produce NH_3. This process is fundamentally different from that of the monocyclic diammonium dinitrate salt, PIPDN, where the second major step retains the cyclic ring and involves nitrosation of the amine nitrogen atoms. DNOP is the product. A blend of these two patterns is found with the bicyclic tertiary amine, DABCOD. Both C–N bond fission and ring retention occur. C–N fission occurs along with α-carbon oxidation leading to CH_2O from one of the ethylene bridges, while the remaining two are retained as a piperazine ring which is nitrosated to form DNOP.

The reaction patterns of these salts resemble those of the mono-, di- and trialkylammonium mononitrate salts(1), such as $[(CH_3)_xNH_{3-x}]NO_3$, x = 1–3. Therefore, we believe that they are general reactions for alkylammonium nitrate salts.

6. References

(1) T. P. Russell and T. B. Brill, *Propellants, Explos., Pyrotech.,* in press.

(2) B. M. Dobratz, Technical Report LA-9732-H, Los Alamos National Laboratory, Los Alamos, NM, May, 1983.

(3) J. T. Cronin and T. B. Brill, *Appl. Spectrosc. 41,* 1147 (1987).

(4) Y. Oyumi and T. B. Brill, *Combust. Flame 62,* 213 (1985).

(5) All computations used SHELXTL (5.1) software written by G. S. Sheldrick, Nicolet XRD, Madison, WI.

(6) T. P. Russell and T. B. Brill, *Combust. Flame 76,* 393 (1989).

(7) A. J. B. Robertson, *J. Soc. Chem. Ind. (London) 67,* 221 (1948).

(8) Y. Oyumi and T. B. Brill, *Combust. Flame 62,* 233 (1985).

(9) M. V. George and G. F. Wright, *J. Am. Chem. Soc. 80,* 1200 (1958).

(10) J. F. Hoffsommer, D. J. Glover, and W. L. Elban, *J. Energ. Mater. 3,* 149 (1985).

(11) R. Behrens, *CPIA Publ. 476(I),* 333 (1987).

(12) J. H. Boyer and T. P. Pillai, *J. Chem. Soc., Perkin. Trans. I,* 1661 (1985).

(13) G. H. Davis, M. M. Demek, and D. H. Rosenblatt, *J. Am. Chem. Soc. 94,* 3321 (1972).

Acknowledgements

We are grateful to the Air Force Armament Laboratory for support of this work on F08635-87-0131 and to Dr. Robert L. McKenney, Jr., for his comments and encouragement.

(Received August 3, 1989; Ms 35/89)